SWEENEY CONVENTION CENTER / SANTA FE / NEW MEXICO
3 - 5 JUNE 1992

Rock Mechanics
Proceedings of the
33rd U.S. Symposium

Edited by
J.R.TILLERSON & W.R.WAWERSIK
Sandia National Laboratories, Santa Fe

OFFPRINT

A.A.BALKEMA / ROTTERDAM / BROOKFIELD / 1992

Rock Mechanics, Tillerson & Wawersik (eds) © 1992 Balkema, Rotterdam. ISBN 90 5410 045 1

Elastic interface waves along a fracture: Theory and experiment

Laura J. Pyrak-Nolte, Jianping Xu & Guy M. Haley
Department of Earth & Atmospheric Sciences, Purdue University, West Lafayette, Ind., USA

Abstract: Laboratory measurements of elastic interface waves were made using a synthetic fracture in an aluminum specimen. Elastic interface waves were observed for shear wave polarization perpendicular to the fracture plane but not for shear wave polarization parallel to the fracture plane. Group velocities of the elastic interface waves were measured as a function of stress on the sample. The group velocities of both interface waves increased with increasing stress. The specific stiffness of the synthetic fracture in aluminum is predicted using the measured group velocities of both interface waves.

1 INTRODUCTION

Fractures play a key role in underground structures and processes. Locating and characterizing fractures by seismic techniques is therefore of great importance to mine stability, production of energy sources in fractured reservoirs, waste isolation, and the study of earthquakes. Though fractures in the Earth are widespread, fundamental issues about their properties must still be addressed. An example is the existence of elastic interface waves along a fracture. A Stoneley wave (Stoneley, 1924) is an elastic interface wave that can travel along a welded interface, i.e., an interface across which stresses and displacements are both continuous. However, a fracture is a non-welded interface, i.e., an interface across which stresses are continuous but displacements are discontinuous. The discontinuity in fracture displacement has been measured quasi-statically in the laboratory by several investigators for normal and shear displacements (Goodman, 1976; Bandis et al., 1983; Swan, 1983; Brown & Scholz, 1985; Yoshioka & Scholz, 1989). The displacement discontinuity model considers a non-welded interface for wave propagation across a fracture. From this purely elastic model, transmission and reflection coefficients, and group velocities are derived which depend on the frequency of the excitation signal and the ratio of fracture specific stiffness (stress per length) to the seismic impedance of the half-spaces. The displacement discontinuity model has been found to reproduce the effects of fractures on wave propagation for both synthetic fractures (Myer et al., 1985; Pyrak-Nolte et al., 1990a) and natural fractures in rock (Pyrak-Nolte et al, 1990b). In this paper, the theory for existence of elastic interface waves propagating along a fracture will be presented and compared with direct observations on a synthetic fracture in the laboratory.

2 THEORY

The existence of elastic interface waves travelling along a fracture is derived by modeling the fracture as a non-welded interface. A non-welded interface is described theoretically by a set of boundary conditions: stress (τ) across the interface is continuous ($\tau_1 = \tau_2$) but the displacements (u) across the interface are discontinuous ($\Delta u = u_1 - u_2 = \tau/\kappa$, where κ is the specific stiffness of the fracture). Several investigators have used these boundary conditions to study wave propagation transmitted across or reflected from a fracture or sets of fractures (Kendall & Tabor, 1971; Schoenberg, 1980 & 1983, Pyrak-Nolte et al., 1990a&b). The displacement discontinuity boundary conditions were applied to two generalized Rayleigh waves traveling in the half-spaces on either side of the fracture assuming discontinuity in both normal and tangential displacements (Pyrak-Nolte & Cook, 1987). Existence of elastic interface waves along a fracture is determined by finding the velocity for which the following determinant is equal to zero (assuming the material properties of each half-space are equal).

$$\begin{vmatrix} c^2 - 2\beta^2 & -(c^2 - 2\beta^2) & -2\beta^2\left(1 - \frac{c^2}{\beta^2}\right)^{1/2} & 2\beta^2\left(1 - \frac{c^2}{\beta^2}\right)^{1/2} \\ \left(1 - \frac{c^2}{\alpha^2}\right)^{1/2} & \left(1 - \frac{c^2}{\alpha^2}\right)^{1/2} & \left(2 - \frac{c^2}{\beta^2}\right)^{1/2} & \left(2 - \frac{c^2}{\beta^2}\right)^{1/2} \\ \left(1 - \frac{c^2}{\alpha^2}\right)^{1/2} - \left(\frac{k\rho}{\kappa_z}\right)(c^2 - 2\beta^2) & \left(1 - \frac{c^2}{\alpha^2}\right)^{1/2} & 1 + \left(\frac{2k\beta^2\rho}{\kappa_z}\right)\left(1 - \frac{c^2}{\beta^2}\right)^{1/2} & 1 \\ 1 + \left(\frac{2k\beta^2\rho}{\kappa_x}\right)\left(1 - \frac{c^2}{\alpha^2}\right)^{1/2} & -1 & \left(1 - \frac{c^2}{\beta^2}\right)^{1/2} + \left(\frac{k\rho}{\kappa_x}\right)\left(2 - \frac{c^2}{\beta^2}\right) & -\left(1 - \frac{c^2}{\beta^2}\right)^{1/2} \end{vmatrix}$$

where

α - compressional wave velocity
β - shear wave velocity
κ_x - shear specific stiffness
κ_z - normal specific stiffness
ω - angular frequency
c - interface wave phase velocity
ρ - density
k - wave number (ω/c)

Table 1. Parameters assumed for modeling elastic interface waves	
Density	2700 kg/m^3
Compressional Wave Velocity[1]	6476.2 m/s
Shear Wave Velocity[1]	3120.6 m/s
Frequency	1.0 MHz

[1]Measured

Two waves were found to exist: a fast and a slow wave. The existence of both waves depends on the specific stiffness of the fracture, the frequency of the excitation signal, and the physical properties of the material on either side of the fracture (which for a fracture are taken to be equal). Both waves are dispersive and the velocities of both waves range between the Rayleigh wave velocity and the shear wave velocity. Figure 1 is a graph of the phase velocity for both waves as a function of fracture specific stiffness, based on the density of aluminum, and the measured compressional and shear wave velocities of the aluminum specimen (Table 1). The interface wave velocities approach the shear velocity with increasing fracture specific stiffness. For low values of fracture specific stiffness, the phase velocity of each wave approaches the Rayleigh wave velocity. Neither waves exist when the transverse component of the elastic wave is

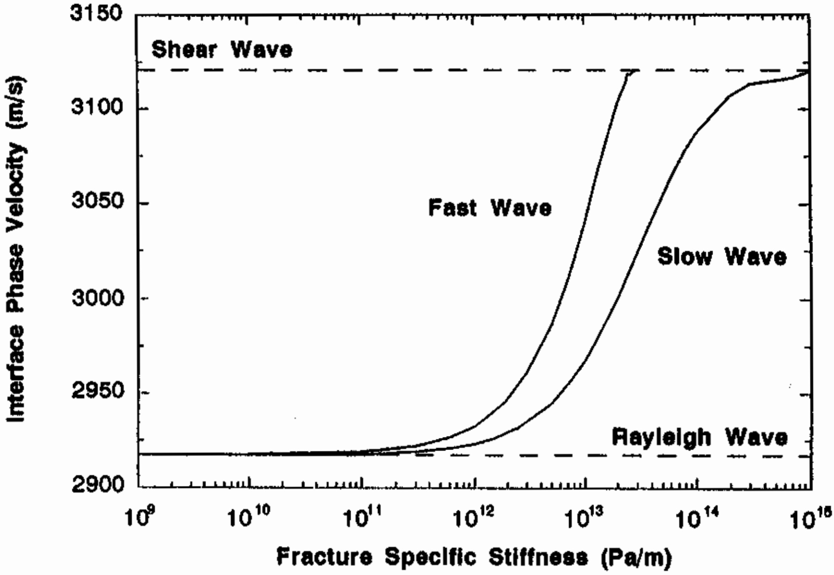

Figure 1. Phase velocity as a function of fracture specific stiffness for the fast and slow interface waves. (Based on parameters in Table 1)

parallel to the fracture plane. These waves are not Stoneley waves, because a Stoneley wave does not exist if the material properties on either side of the interface are identical. The particle motion of each wave is shown in Figure 2 as a function of distance from the fracture. Both waves have prograde particle motion. The slow wave is in phase in the direction parallel to the fracture plane and thus only sensitive to changes in shear stiffness, while the fast wave is in phase in the direction perpendicular to the fracture and thus is only sensitive to changes in the normal stiffness.

3 EXPERIMENTAL SET-UP

To measure elastic interface waves that propagate along a fracture, a synthetic fracture was made in a cylinder of aluminum (29.3 cm diameter by 29.3 cm high). Aluminum was chosen because of its low attenuation. Before cutting the aluminum to form the fracture, compressional and shear wave velocities were measured on the intact specimen. The synthetic fracture was made by cutting the aluminum in half, planing down the surfaces and then sandblasting the surfaces with 300 μm grit to roughen the surfaces.

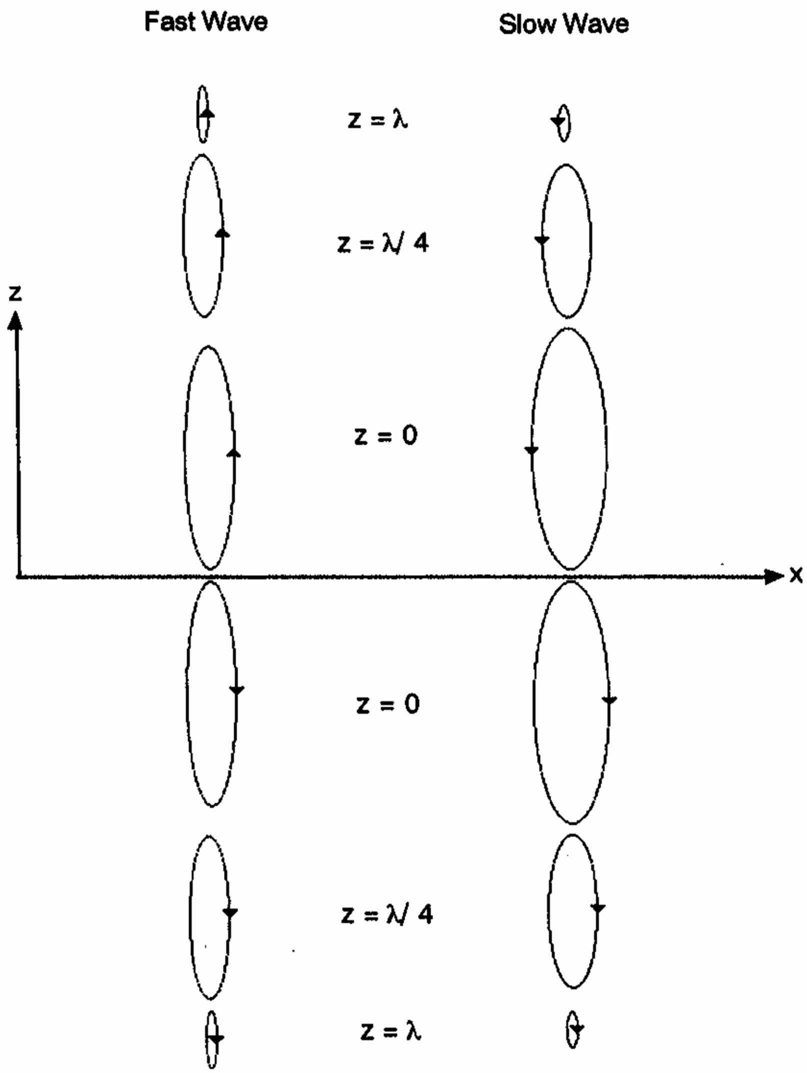

Figure 2. Particle motion of fast and slow interface waves for increasing depth from the interface.

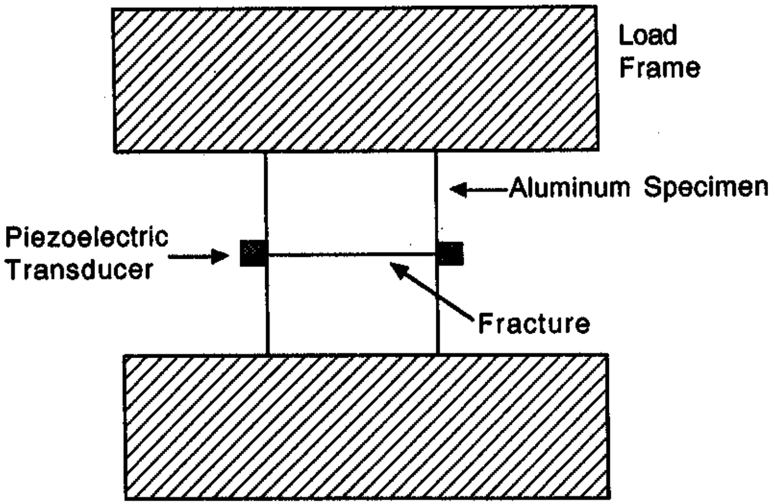

Figure 3. Experimental geometry for measuring interface waves.

Figure 3 is a diagram of the experimental set-up. Shear wave piezoelectric crystals (1 MHz resonant frequency) were mounted diametrically opposed straddling the fracture. The shear wave particle motion is perpendicular to the fracture plane (0°). The transducers were excited with a 1000 V spike 0.3 μs in duration at a repetition rate of 100 cycles/sec. The received signal was sent to a digital oscilloscope and the data were collected by computer. To change the stiffness of the fracture, the aluminum specimen was placed in a load frame and subjected to a range of stresses (0 MPa to 30 MPa). Measurements were also made for shear wave polarizations of 90° (parallel to the fracture plane) and at 45°.

4 RESULTS

Figure 4 shows the received waveforms for shear wave particle motions of 0° and 90°. An interface wave is observed for 0° and arrives 5.92 microseconds after the arrival of the shear wave at 94.80 microseconds. The amplitude of the shear wave relative to the amplitude of the interface wave indicates that there is almost complete coupling of the transducer energy into the interface wave. For a shear wave orientation of 90°, no interface wave is observed to exist, as predicted by the theory. For an orientation of 45°, the shear wave and interface wave have nearly equal amplitudes.

The effect of fracture specific stiffness on elastic interface waves was examined by applying normal stress to the specimen to change the fracture specific stiffness. Figure 5 contains the received waveform (0° orientation) when the specimen is subjected to 3 MPa and 13.2 MPa. At 3 MPa only one interface wave is observed which arrives 5.22 microseconds after the shear wave arrival. At 3 MPa, a broadening of the interface wave is observed, suggesting the emergence of another interface wave. As stress is increased on the aluminum specimen to 13.2 MPa, a second (fast wave) interface

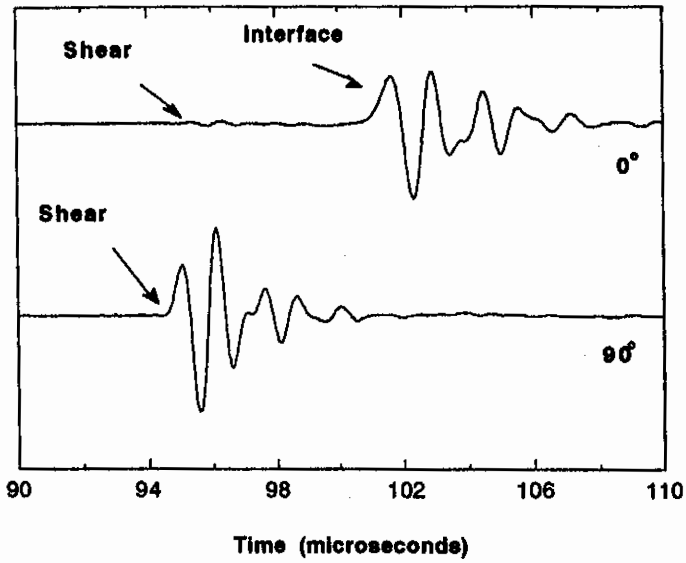

Figure 4. Received waveforms for shear polarizations perpendicular to the fracture plane (0°) and parallel to the fracture plane (90°). No interface wave is observed for a shear wave orientation of 90°.

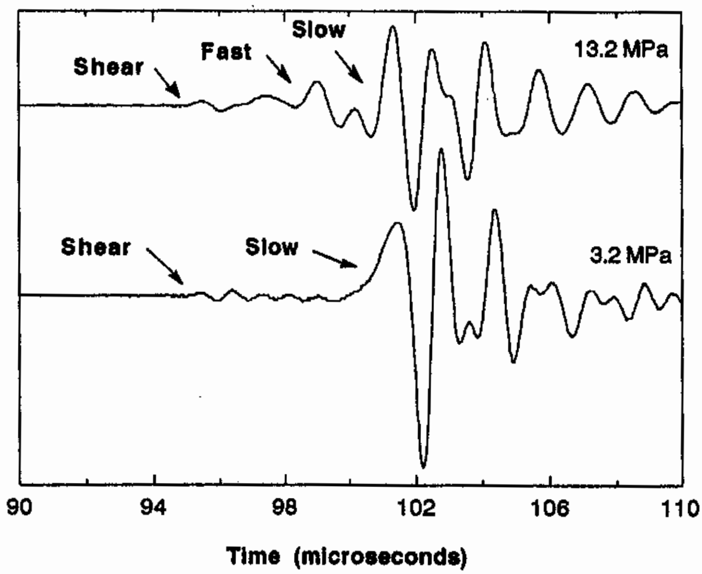

Figure 5. Received waveforms (shear wave orientation 0°) for stresses of 3 MPa and 13.2 MPa for a fracture in aluminum. As the fracture specific stiffness increases because of the increase in normal stress on the fracture, the fast interface wave emerges.

wave is observed. The fast wave arrives 2.12 microseconds after the shear wave arrival (94.78 microseconds) while the slow wave arrives 5.22 microseconds after the shear wave arrival.

The group velocity for the waves is determined from the measured arrival times minus the system delay (0.8μs) divided by the length of the travel path. Figure 6 is a graph of the measured group velocity for the two interface waves and the shear wave for an orientation of 0°. The shear wave velocity remained essentially constant with increasing stress. For both interface waves the group velocity increases with increasing stress.

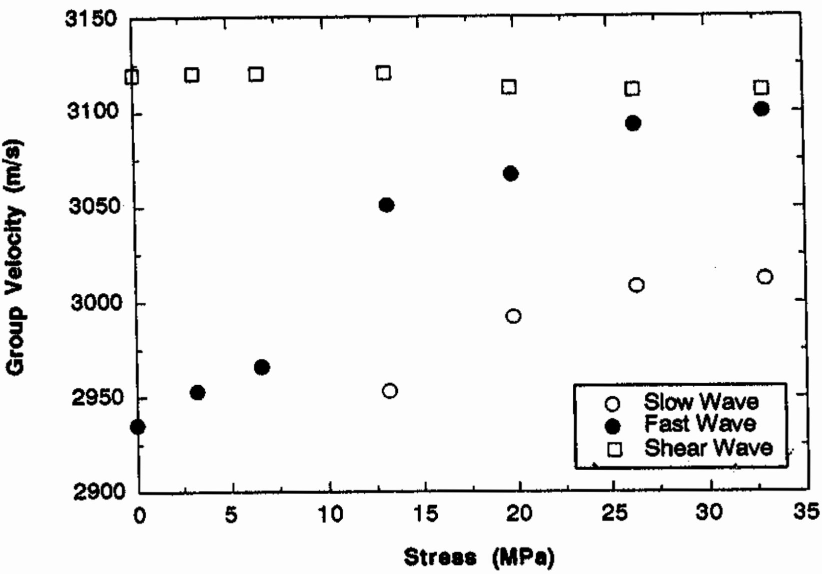

Figure 6. Group velocity of shear wave, slow interface wave, and fast interface wave for a fracture in an aluminum specimen as a function of normal stress on the specimen.

5 ANALYSIS

From the theory, it was determined that the slow wave is only sensitive to changes in shear stiffness of the fracture and the fast is sensitive only to changes in the normal fracture stiffness. From the experimental data, the shear and normal stiffness of the fracture can be predicted using the theory for elastic interface waves propagating along a fracture. Because group velocities are measured in the experiment, it is necessary to calculate theoretical values of group velocity. If a wave is non-dispersive then the group velocity is equal to the phase velocity. However, the elastic interface waves are dispersive and the group velocity is calculated based on $\Delta\omega/\Delta k$ for small increments in frequency ($\Delta f = 200$ Hz). Figure 7 shows the theoretical curves of group velocity as a function of fracture stiffness for the parameters listed in Table 1. In comparing the phase velocity (Figure 1) and group velocity (Figure 7) of the elastic interface waves, the group velocity is lower in value than the phase velocity for a constant value of fracture stiffness.

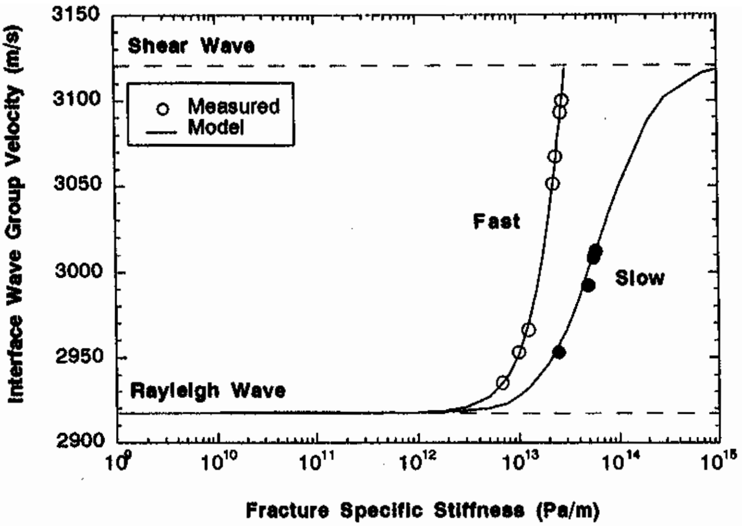

Figure 7. Theoretical and measured group velocities as a function of fracture specific stiffness.

In Figure 7, the measured values of group velocity are plotted on the theoretical curves from which the normal and shear stiffness of the fracture is predicted. Table 2 gives the values of the shear and normal stiffness predicted by the theory as a function of stress. Both shear and normal fracture stiffness increased with increasing stress. Fracture stiffness normal to the fracture plane is smaller in value than the shear fracture stiffness.

Table 2. Predicted values of normal and shear fracture specific stiffness based on measured values of velocity.

Stress (MPa)	Normal Stiffness (10^{12} Pa/m)	Shear Stiffness (10^{12} Pa/m)
0	6.8	
3.2	10.0	
6.6	12.5	
13.2	22.5	25.0
19.8	23.8	50.0
26.3	27.0	56.0
32.9	28.1	60.0

6 CONCLUSION

Elastic interface waves were observed in a synthetic fracture in aluminum. From measurements of the group velocities of the waves, fracture specific stiffnesses were predicted for the fracture. For an incident shear wave with particle motion perpendicular to the fracture, there is almost complete coupling of the energy into the elastic interface. No interface waves are observed for shear wave particle motion parallel to the fracture, as predicted by the theory. The observation of this wave represents a further validation of the displacement discontinuity model for modeling wave propagation in a fracture medium. The experimental observation of this wave may result in the reinterpretation of laboratory and field data. In addition, the observation of the elastic waves suggests that with further development, this wave could be used to characterize natural fractures and hydraulic fractures in situ.

Acknowledgment: This work was supported by the National Science Foundation grant EAR-9021644. The authors wish to thank ALCOA for the donation of the aluminum specimen, Russ Maury for running the hydraulic press, and D.D. Nolte for use of equipment.

References

Bandis, S.C., A.C. Lumsden & N.R. Barton 1983. Fundamentals of rock joint deformation. Int. J. Rock Mech. Min. Sci. Geomech. Abstr. 20:249-268.

Brown, S.R. & C.H. Scholz 1985. Closure of random surfaces in contact. J. Geophys. Res. 90:5531-5545.

Goodman, R.E. 1976. Methods in Geological Engineering. West Pub. Co. St. Paul. 170-173.

Kendall, K. & D. Tabor 1971. An ultrasonic study of the area of contact between stationary and sliding surfaces. Proc. Roy. Soc. (London) A. 323:321-340.

Myers, L.R., D. Hopkins & N.G.W. Cook 1985. Effects of contact area of an interface on acoustic wave transmission characteristics. In research Engineering Applications in Rock Masses. edited by E. Ashworth. A.A Balkema. Boston, Mass. 1:565-572.

Pyrak-Nolte, L.J. & N.G.W. Cook. 1987. Elastic interface waves along a fracture. Geophys. Res. Let. 14:1107-1110.

Pyrak-Nolte, L.J., L.R. Myer & N.G.W. Cook 1990a. Anisotropy in seismic velocities and amplitudes from multiple parallel fractures. J. Geophys. Res. 95:11345-11358.

Pyrak-Nolte, L.J., L.R. Myer & N.G.W. Cook 1990b. Transmission of seismic waves across single natural fractures. J. Geophys. Res. 95:8617-8638.

Schoenberg, M. 1980. Elastic wave behavior across linear slip interfaces. J. Acoust. Soc. Am. 68:1516

Schoenberg, M. 1983. Reflection of elastic waves from periodically stratified media with interfacial slip. Geophys. Prospect. 31:265-292.

Stoneley, R. 1924. Elastic waves at the surface of separation of two solids. Proc. Roy. Soc. (London) A. 106:416-428.

Swan, G. 1983. Determination of stiffness and other joint properties from roughness measurements. Rock Mech. Rock Eng. 16:19-38.

Yoshioka, N. & C.H. Scholz 1989. Elastic properties of contacting surfaces under normal and shear loads 2. Comparison of theory with experiment. J. Geophys. Res. 94:17691-17700.